Electronic Supplementary Material (ESI) for RSC Advances.
This journal is © The Royal Society of Chemistry 2016

Hierarchical self-assembled nanoclay derived mesopours CNT/polyindole electrode for supercapacitors

Ramesh Oraon[a], A. De Adhikari[a], Santosh Tiwari[a], S. Bhattacharya[b] and Ganesh Chandra Nayak[a*]

[a]Dept. of Applied chemistry, ISM Dhanbad, Dhanbad 826004, Jharkhand, India

[*]Corresponding Authors: nayak.g.ac@ismdhanbad.ac.in

Number of Pages: 10

Number of figures: 10

Number of tables: 2

Electronic Supporting Information

1. ***Cyclic Voltammetry study in 1M aq. KCl solution at higher scan rates:***

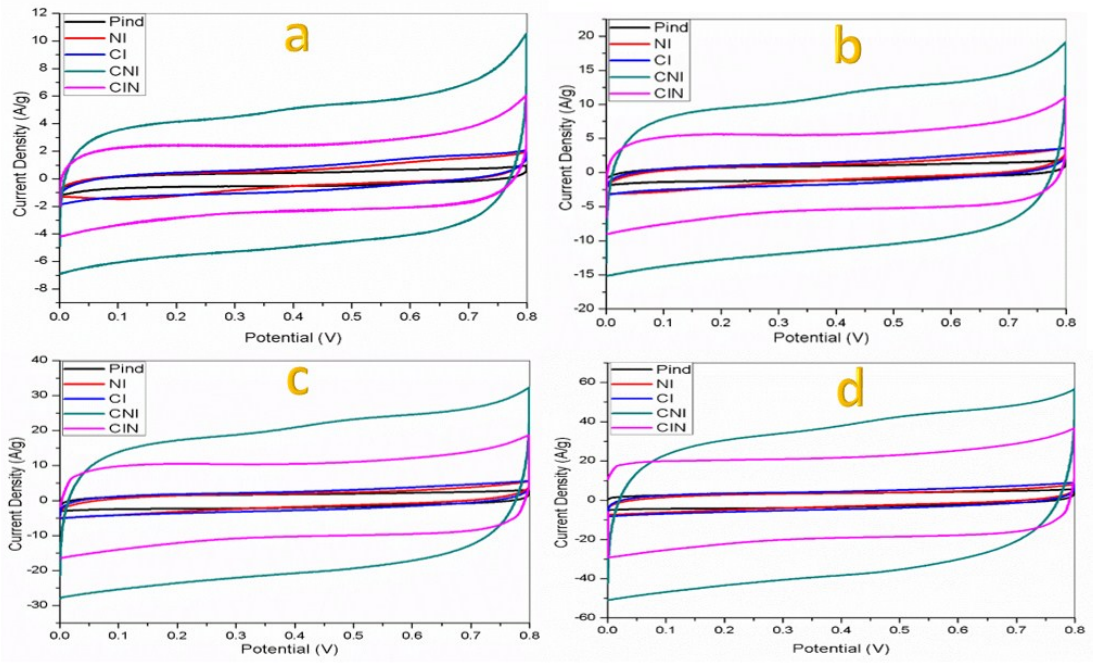

Figure S1: Cyclic Voltammetry study of different sample at higher scan rates (a) 20 mV/s (b) 50 mV/s (c) 100 mV/s (d) 200 mV/s

2. ***DC conductivity measurement of nanoclay based ternary electrode material:***

Four probe measurement technique (by Keithley 2400 SMU) was employed to investigate the electrical properties of as prepared nanoclay based ternary in-situ & ex-situ nanocomposite. Calculation were done using the following formula:

$$\text{Resistivity } (\rho \text{ Ohm-cm}) = (4.532\ V\ t)/\ I \quad \text{Ref: 1}$$

Where, V = Applied Voltage, t = thickness, I = Measured current through the sample

$$\text{Conductivity } (\sigma \text{ S/cm}) = 1/\ \rho$$

Where, σ = Conductivity, ρ = Resistivtiy

It was found that ex-situ CIN exhibited maximum electrical conductivity of 0.071 S/cm which further increases to 6.06 S/cm for in-situ CNI. This enhanced electrical conductivity of in-

situ CNI could be ascribed to formation of high surface area and 3D interconnected conductive framework of nanocomposite which is the consequence of in-situ incorporation of nanoclay to CI system. In our case in-situ incorporation of nanoclay after Pind coating provides a conductive pathway in between CNT/Pind and increase the overall electronic conductivity which is evidenced from the absence of non-linearity of I-V curves [Ref.2]. On the other hand, non-linearity of CIN in I-V curves suggests the semi-conducting behavior and non-deterioration property of nanoclay in conductivity of sample. Their electrical properties are tabulated below:

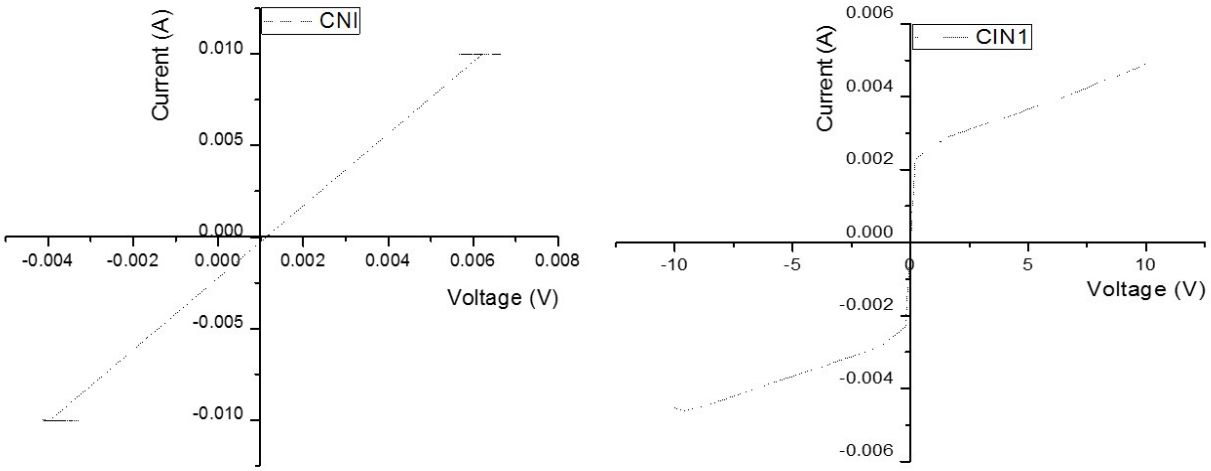

Figure S2: Characteristic I-V curves of in-situ CNI and ex-situ CIN nanocomposite

Table 1: Electrical Conductivity Measurements

Sample	d (in cm)	Resistance (Ω)	ρ (Ω-cm)	σ (S/cm)
CNI	0.1	0.364	0.1649	**6.06**
CIN	0.1	30.71	13.91	**0.071**

Reference:

1. C. Harish, V. S. Sreeharsa, C. Santosh, R. Ramachandran, M. Saranya, T. M. Vanchinathan, K. Govardhan, A. N. Grace. Synthesis of polyaniline/Graphene nanocomposite and its optical, electrical and electrochemical property. Advance Science Engineering and Medicine. 4, 2012, 1-9

2. A. B. Oskouyi, U. Sundararaj, P. Mertiny. Tunnelling Conductivity and Peizoresistivity of Composites Containing Randomly Dispersed Conductive Nano-Platelets. Materials. 2014, 7, 2501-2521

3. Cyclic Voltammetry study in the organic electrolyte:

A supercapacitor test cell composing two symmetrical electrodes coated on platinum foil prepared by mixing different sample with PVDF and carbon black in the mass ratio of 85:15:5 in dispersant N-methyl pyrrolidone. These prepared samples were vacuum dried overnight at 80 °C to ensure the exact weight measurement of sample used. For electrochemical analysis, samples coated on symmetrical Pt foil are separated by 1M $TEABF_4$ (tetraethyl ammonium tetrafluoro borate) in acetonitrile absorbed solution in thin filter paper. All electrochemical analysis of samples viz. cyclic voltammetry (CV), Galvanostatic charging-discharging test (GCD), electrochemical impedance spectroscopy (EIS) were performed for two electrode configuration in two potential window ranging from (0-0.8V) & (0-1.6V) and presented in figure S3 (a) & S4 (a), respectively, at scan rate 10 mV/s. All CV curves in both potential window shows non-ideal rectangular shape indicating the formation of typical hybrid composite consisting both EDLCs and pseudocapacitance. It was also observed that ternary nanocomposite (in-situ & ex-situ) exhibited maximum current density as compared to pure Pind and binary nanocomposite (NI & CI). These observations are evident with the higher cyclic enclosed area under voltamogram for ternary nanocomposite which could be ascribed to the doping effect of nanoclay. Specific capacitance (SC), energy density (ED) and power density (PD) were calculated using the following formulae:

$$SC = \left(4 \int_{V-}^{V+} I(V)dv\right) / m\Delta Vv \quad \ldots\ldots\ldots\ldots\ldots\ldots\ldots\ldots (1)$$

Where, m= mass of the active sample, v= scan rate, ΔV= voltage window

$$ED = \tfrac{1}{2} CV^2 \quad \ldots\ldots\ldots\ldots\ldots\ldots\ldots\ldots\ldots\ldots\ldots\ldots\ldots\ldots (2)$$

Where, C=specific capacitance in (F/g), V= Potential window

$$PD = E/t \quad \ldots\ldots\ldots\ldots\ldots\ldots\ldots\ldots\ldots\ldots\ldots\ldots\ldots\ldots (3)$$

Where, E= Energy Density in (Wh/Kg), t= time in second

Calculations revealed that maximum specific capacitance was achieved for in-situ (428.5 F/g) & ex-situ (263 F/g) ternary nanocomposite which is comparatively higher as compared to pure Pind (26.87 F/g) and binary nanocomposite (NI~62.5) & (CI~158 F/g), respectively. These results suggests that incorporation of nanoclay is expected to increase the overall specific capacitance of CNT/Pind system. These results are in good agreement with the increased capacitance value of NI

and in-situ & ex-situ nanocomposite as compared to pure Pind and binary nanocomposite CI, respectively and follow the similar trend for energy density and power density. The corresponding bar plots of SC, ED and PD are shown in figure S3 (b):

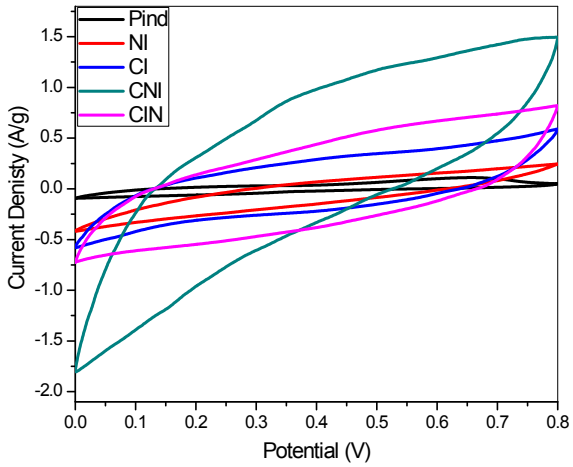

Figure S3 (a): Comparative current density plot of different sample at 10 mV/s

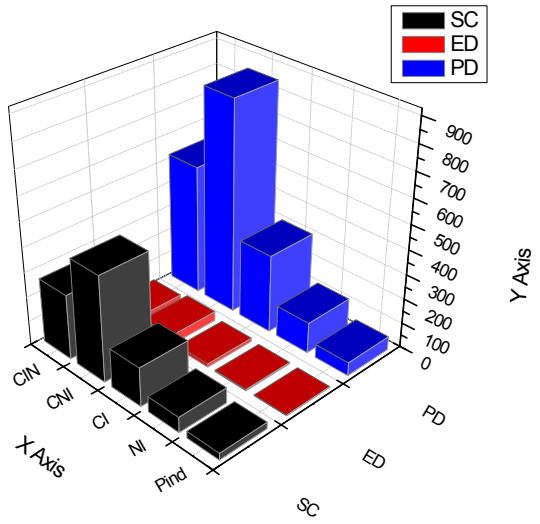

Figure S3 (b): Comparative bar plot of different sample at 10 mV/s

It should also be mentioned that these capacitance values in organic electrolyte ($TEABF_4$/Acetonitrile) are lower in comparison with capacitance values in aq. 1M KCl solution. From fundamental point of view results are well consistent for prepared sample. Since bigger ionic size of organic electrolyte can circumvent the ionic mobility during electrochemical analysis which consequently leads to lower electrochemical performance. However, to improve their performance cyclic voltammetry analysis was further performed for extended potential (0-1.6V) and presented in figure S3 (a). It was found that all samples retains similar potentio-dynamic behavior while maintaining higher current density than in (0-0.8V). These observation also document the high rate capability and high stability of as prepared nanocomposite. Electrochemical measurements

carried out for two electrode configuration revealed that ternary nanocomposite (in-situ ~582.5 F/g) & (ex-situ~433.83 F/g) showed higher capacitance values than pure Pind (53.63 F/g) and binary nanocomposite (NI~75.33) & (CI~158 F/g), respectively. Meanwhile, among nanoclay based ternary nanocomposite in-situ (201 Wh/g) found to deliver higher energy density than ex-situ (154 Wh/Kg) at the power density of 2330 W/Kg and 1733 W/Kg, respectively. Higher capacitance values of in-situ product as compared to ex-situ product revealed that in-situ incorporation of nanoclay results in much improved electrochemical property (like electrical conductivity) and electron hopping within electrode than in ex-situ composite.

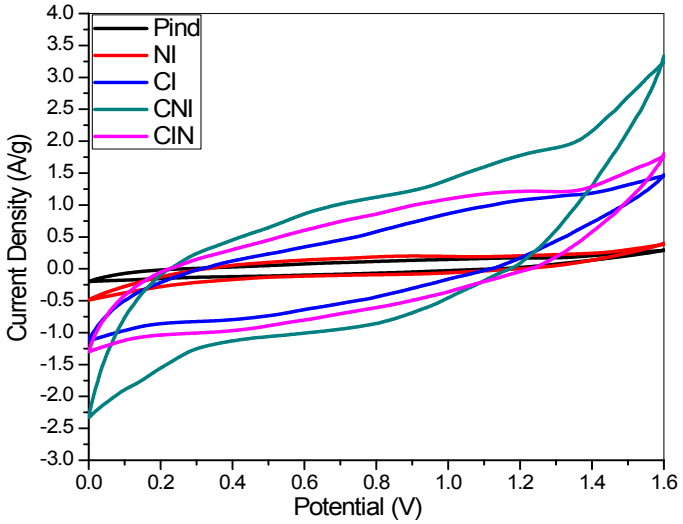

Figure S4 (a): Comparative current density plot of different sample at 10 mV/s

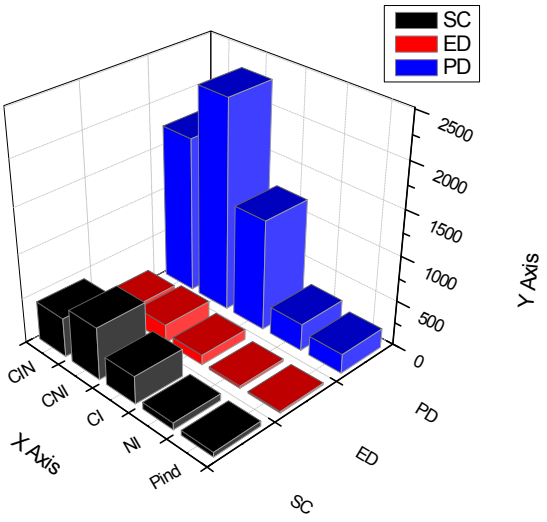

Figure S4 (b): Comparative bar plot of different sample at 10 mV/s

4. Galvanostatic charging discharging Analysis:

To complement the CV analysis and their results, charging discharging analysis was further performed in organic electrolyte ($TEABF_4$/Acetonitrile) for two electrode configuration at 2.5 A/g. Two potential window was remained same as in case of CV analysis and presented in figure S5 (a & b).

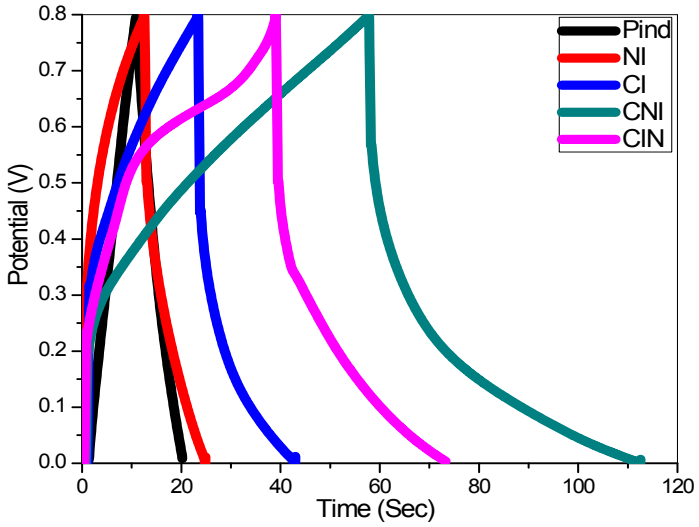

Figure S5 (a): Galvanostatic charging discharging test of different sample within potential window (0-0.8V) at 2.5 A/g

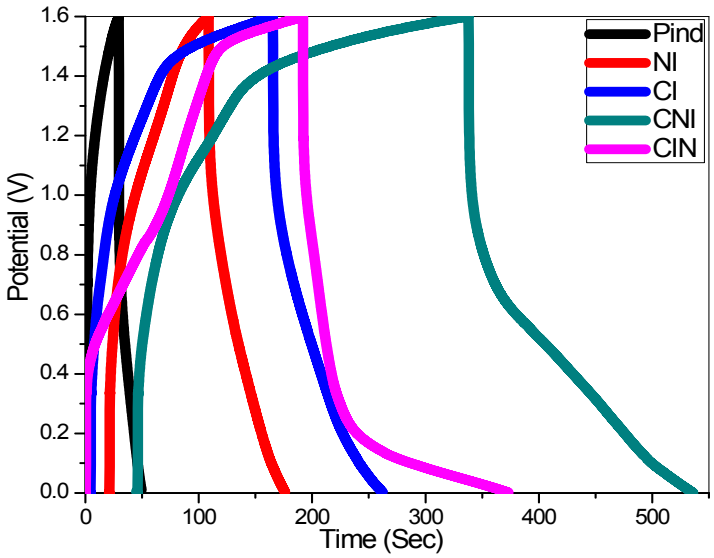

Figure S5 (b): Galvanostatic charging discharging test of different sample within potential window (0-1.6V) at 2.5 A/g

It is noted that in both potential window all curves shows deviation from linearity which demonstrates charge storage from both EDLCs and pseudocapacitance while maintaining the

characteristics of typical hybrid nanocomposite. Fundamentally larger discharge time signifies the high capacitive performance which is notified in case of ternary nanocomposite (in-situ & ex-situ) as compared to other related systems. It was observed discharge time including deviation from linearity was increased after nanoclay incorporation for both pure Pind and binary nanocomposite. Similar doping effect of nanoclay can be ascribed to their enhanced electrochemical performance in terms of larger discharge time duration. Specific capacitance of all sample at 2.5 A/g was calculated using the following formula:

$$\text{Specific capacitance (SC)} = (I\Delta t/m\Delta V)\ldots\ldots\ldots (4)$$

Where, I = Applied current (A), Δt = discharge time (sec), m = Mass (g), ΔV = Potential

$$ED = \tfrac{1}{2} CV^2\ldots\ldots\ldots\ldots\ldots\ldots\ldots\ldots\ldots\ldots\ldots..(2)$$

Where, C=specific capacitance in (F/g), V= Potential window

$$PD = E/t\ldots\ldots\ldots\ldots\ldots\ldots\ldots\ldots\ldots\ldots\ldots..(3)$$

Where, E= Energy Density in (Wh/Kg), t= Discharge time (sec)

Similar to CV analysis charging discharging analysis at the current density of 2.5 A/g, ternary in-situ (350 F/g) & ex-situ (230 F/g) nanocomposite showed much higher specific capacitance as compared to other related system like pure Pind (31.25 F/g) and binary nanocomposite (NI~75 F/g) & CI (130 F/g), respectivley. In-situ CNI offered highest energy density of (31 Wh/Kg) at the power density of (700 W/Kg). However, these values are observed to be enhanced after the extension of potential window upto (0-1.6V). In case of ternary nanocomposite specific capacitance values are increased for in-situ (762.5 F/g) and ex-situ (585 F/g), respectively. Similar trend was also observed for pure Pind (76.4 F/g) and binary nanocomposite NI (106.25 F/g) & CI (402 F/g), respectivley. Thus, all such observation further confirms the high stability of as prepared nanocomposite at higher potential window with improved electrochemical performance. Among all, in-situ nanocomposite CNI exhibited maximum energy density (271 Wh/Kg) at the power density of (3037.5 W/Kg) at same current denisty 2.5 A/g.

5. *Electrochemcial Impedance Spectroscopy (EIS) study:*

Corresponding Nyquist plot of as prepared nanocomposites were further interpreted by fitting the experimental data with equivalent electrical circuit. Equivalent circuit is shown schematically in figure S6 and their fitted curves and values are given below as follow:

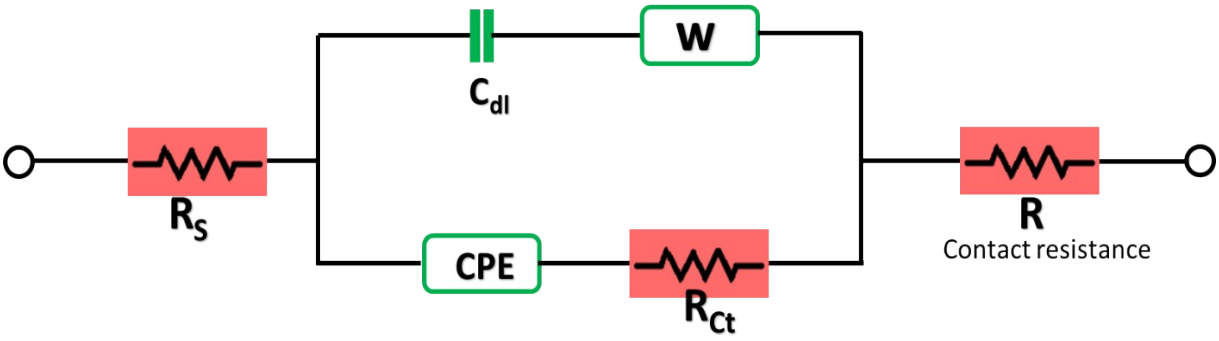

Figure S6: Equivalent circuit used for the fitting of Nyquist plots

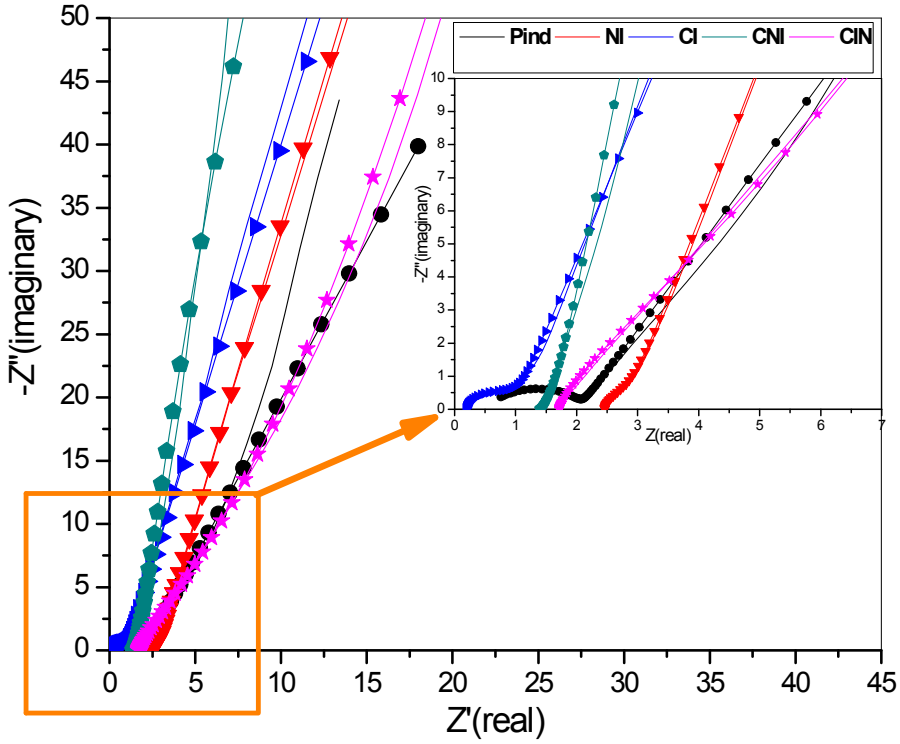

Figure S7: Fitting of corresponding Nyquist plot of as preapred nanocomposite

Table 2: Fitted value of Equivalent circuit element obtained by the simulation of impedance spectra

Sample	R_s + Rcontact (Ω)	C_{dl}	R_{ct}(Ω)	W	CPE	n
Pind	(0.0668+0.382)	$5.80e^{-5}$	1.611	0.0038	0.0051	0.75
NI	(0.0018+2.364)	0.0001	0.0277	0.02271	0.00639	0.5
CI	(0.0021+0.176)	0.0001	1.03	0.257	0.00218	0.85
CNI	(0.00104+1.703)	0.0025	0.00813	0.0093	0.00027	0.983
CIN	(0.0008+1.383)	0.0012	0.01	0.081	0.000637	0.55